

Supporting Information:

Micro-Solid State Energy Conversion Membranes: Influence of Doping Concentration and Strain on Oxygen Transfer and Near Order for Electrolytes

Yanuo Shi¹, Iñigo Garbayo¹, Paul Murali², Jennifer Lilia Marguerite Rupp¹

¹ Electrochemical Materials, Department of Materials, ETH Zürich, Switzerland

² Ceramics Laboratory, Ecole Polytechnique Fédérale de Lausanne EPFL, Lausanne, Switzerland

Correspondence should be addressed to J.L.M.R.

S1: The fabrication of free standing electrolyte membranes with microelectrodes

Fig. S1 illustrates the fabrication process of free-standing membrane samples. The consecutive steps in the fabrication flow are (i.) coating of Si_3N_4 layers on the two sides of a silicon wafer by low pressure chemical vapor deposition (LPCVD), (ii.) photolithography to define the area to be etched via reactive ion etching (RIE) for releasing the Si_3N_4 layers from Si on the back side, (iii.) wet etching with KOH from the back side to remove the Si substrate and get free-standing Si_3N_4 membrane, (iv.) PLD to obtain a ceramic oxide layer on top of Si_3N_4 , (v.) a 2nd RIE step to etch the Si_3N_4 underneath the doped ceria layer, (vi.) Pt deposition by e-beam evaporation patterned by a shadow mask and (vii.) contacting of the top microelectrodes via micropositioners in a microprobe station and attached for electrochemical test.

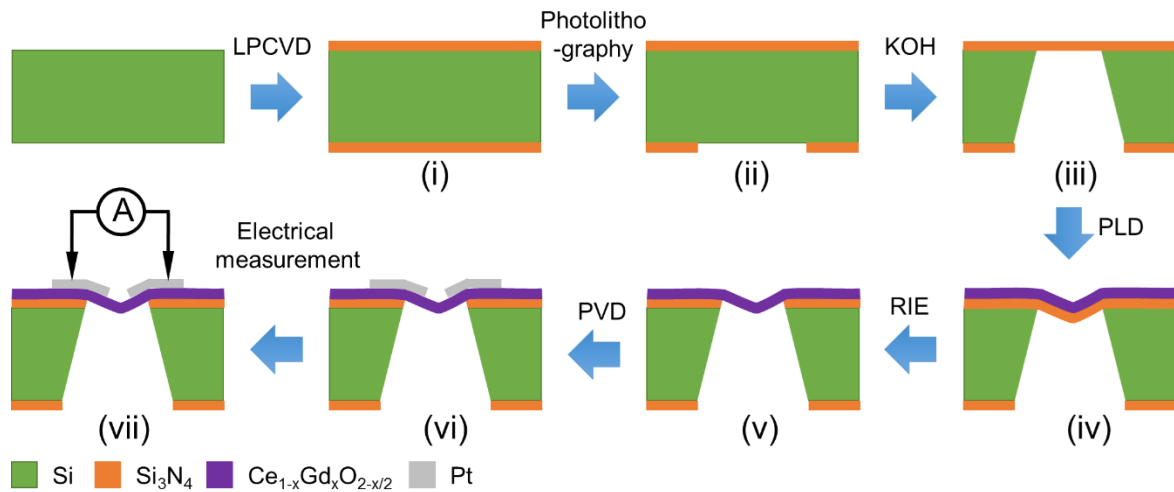


Figure S1: Manufacturing process flow of gadolinia doped ceria free-standing membranes.

S2: The comparison between free standing and substrate-supported gadolinia doped ceria thin films in the full width at half maximum of F_{2g} mode as a function of compressive net strain

Fig. S2 describes the relationship between the full width at half maximum (FWHM) of F_{2g} peak and compressive net strain of different samples. FWHM is frequently used as a measure of the defect density or crystallinity of thin films, i.e. sharper peaks (lower FWHM) correspond to highly crystalline films and/or less defects^{1,2}. In this case, FWHM of the F_{2g} peaks is getting larger with the increasing of doping concentration, as well as when turning the originally flat to the buckled membranes. It is remarkable that the variation between substrate-supported and free-standing thin film is increased with doping concentration.

Here, larger FWHM with the increasing of doping concentration is interpreted as less thin film crystallinity¹, what could be associated to the larger number of defects on the structure. In parallel, buckling membranes were also found to have lower crystallinity than the flat substrate-supported samples, what could be explained by the more compressive strain affecting the microstructure of the thin film.

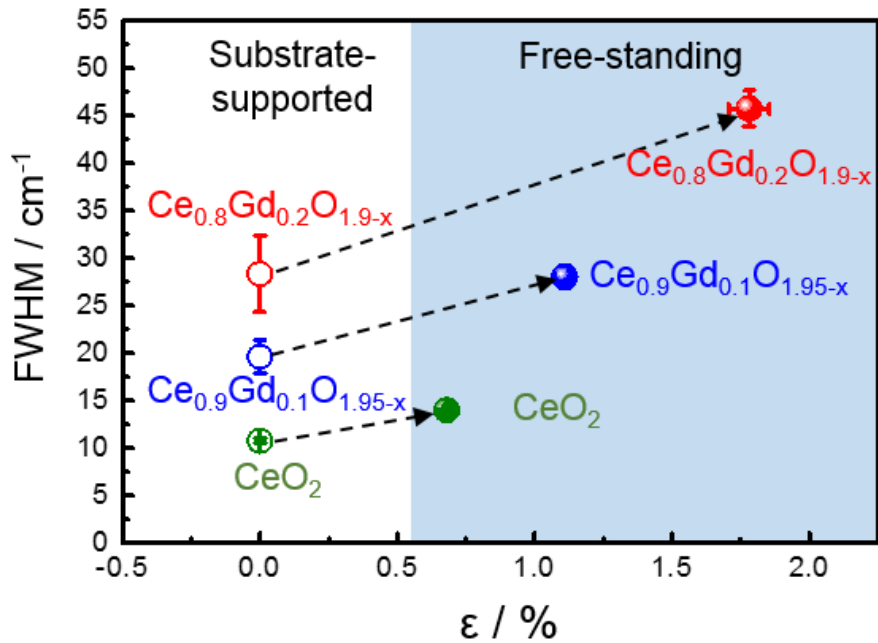


Figure S2: Full width at half maximum of the F_{2g} Raman peak as a function of the net compressive strain calculated by optical profilometry, for free-standing and substrate-supported thin films of the three materials analyzed.

S3: Characterization of the ionic conductivity of the CeO_2 , $Ce_{0.9}Gd_{0.1}O_{1.95-x}$ and $Ce_{0.8}Gd_{0.2}O_{1.9-x}$ thin films: application of impedance spectroscopy

Impedance spectroscopy was used in order to get the ionic conductivity of the doped ceria thin films. For all the samples the measurement was processed between 335 °C to 530 °C, applying an AC voltage of 100 mV. The measuring frequency was varied from 1 MHz to 0.1 Hz. Fig. S3 shows an example of a series of measurements at different temperatures corresponding to a representative $Ce_{0.9}Gd_{0.1}O_{1.95-x}$ free-standing membrane. The whole series of measurements for this particular sample is shown in Fig. S3a in the form of Nyquist plots. Fig. S3b shows a closer look of the Nyquist plots obtained above 450 °C. The equivalent circuit used for fitting is also included as an inset. Three different elements are identified and fitted, i.e. the contribution of bulk (a first semicircle appearing at high frequencies), grain

boundary (a second semicircle at mid frequencies) and the electrode (artifact at low frequencies). For this work, the total resistance of the electrolyte was calculated as the sum of resistances measured for the bulk and grain boundaries.

To confirm the influence of the electrode, all the samples were additionally measured by applying different DC biases³. One instance is shown in Fig. 3c, corresponding with a $\text{Ce}_{0.9}\text{Gd}_{0.1}\text{O}_{1.95-x}$ substrate-supported thin film measured at 578 °C, under 0V and 1V DC bias, respectively. It can be clearly observed how only the part of electrode deviates when DC bias is applied.

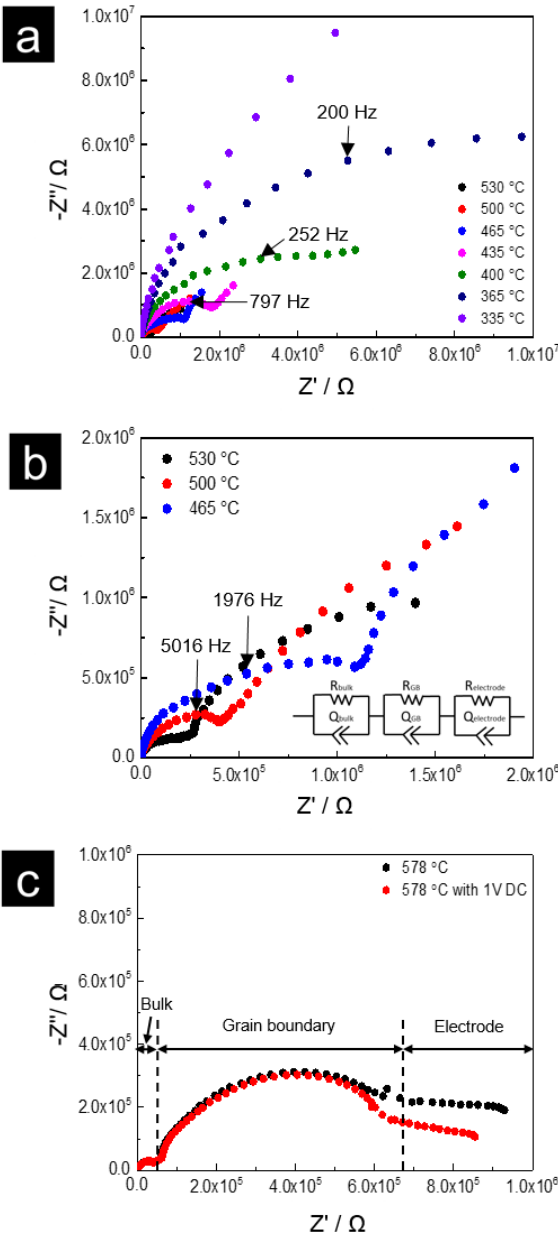


Figure S3: Ionic conductivity measurement through impedance spectroscopy. (a) Nyquist plots of $\text{Ce}_{0.9}\text{Gd}_{0.1}\text{O}_{1.95-x}$ free-standing membrane measured from 335 °C to 530 °C. (b) Close look of plots in figure S3a obtained above 450 °C, where the different contributions to the total resistance can be observed clearer. (c) Example of an impedance measurement on a $\text{Ce}_{0.8}\text{Gd}_{0.2}\text{O}_{1.9-x}$ substrate-supported thin film with different DC biases, to demonstrate the influence of DC bias on the impedance spectra, used to ensure the contribution of electrolyte.

S4: Discussion on the reproducibility of the free-standing thin film and experiment result

One challenge to the experiment based on the free-standing membranes is the survival rate after fabrication. In our experiments there are four thin films in the array of fabricated membranes (Fig 1a in main text). To control the variables and consider the uniformity of the PLD deposition, we only focused on the two membranes in the center of one line. We checked the reliability of the data by measuring the ionic conductivity of different independent membranes with same doping concentration, e.g. $\text{Ce}_{0.8}\text{Gd}_{0.2}\text{O}_{1.9-x}$ free-standing membranes. Firstly, we checked the buckling pattern of two $\text{Ce}_{0.8}\text{Gd}_{0.2}\text{O}_{1.9-x}$ membranes fabricated by the same process, as shown in the Fig. S4a, the buckling pattern of membrane and the out-of-plane amplitudes between the same pairs of diagonal electrodes is nearly same, which reflected the similar strain level and distribution. Then the in-plane ionic conductivity measurement result between the diagonal electrodes is illustrated in Fig S4b. It is found that the ionic conductivities measured from the different membranes are also nearly overlapped with each others, except 1 or 2 points (the biggest variation of ionic conductivity is by a factor of 1.5, much smaller than the difference between the ionic conductivities of the samples in our experiment). This deviation influences the activation energy by $\Delta 0.02$ eV, which is acceptable. Consider the error of the activation energy we reported, we conclude that the experiment result can be reproduced on the other membrane.

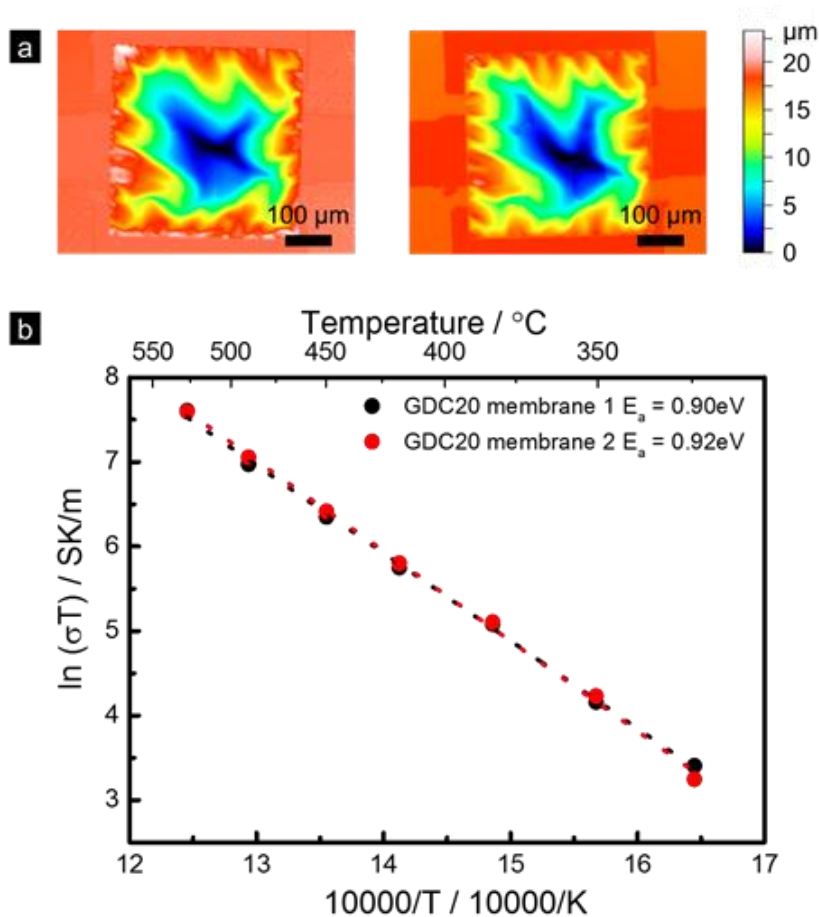


Figure S4: Experiment on the reproducibility of free-standing membranes. (a) Comparison of optical profilometry graphs obtained from two different $\text{Ce}_{0.8}\text{Gd}_{0.2}\text{O}_{1.9-x}$ free-standing membranes with same fabrication process. (b) Ionic conductivity measurement of different $\text{Ce}_{0.8}\text{Gd}_{0.2}\text{O}_{1.9-x}$ membranes through impedance spectroscopy, the ionic conductivity is same.

References

- 1 S. J. Park, K. H. Kim, W. S. Sohn, J. H. Oh and J. Jang, *J. Korean Phys. Soc.*, 2003, **42**, 466–471.
- 2 K. Kitahara, T. Ishii, J. Suzuki, T. Bessyo and N. Watanabe, *Int. J. Spectrosc.*, 2011, **2011**, 1–14.
- 3 J. Fleig, F. S. Baumann, V. Brichzin, H. Kim, J. Jamnik, G. Cristiani, H. Habermeier and J. Maier, *Fuel Cells*, 2006, **6**, 284–292.